Rotational symmetry breaking in $Bi_2Sr_2CaCu_2O_{8+\delta}$ probed by polarized femtosecond spectroscopy

Y. Toda,[1] F. Kawanokami,[1] T. Kurosawa,[2] M. Oda,[2] I. Madan,[3] T. Mertelj,[3] V. V. Kabanov,[3] and D. Mihailovic[3]

[1]*Department of Applied Physics, Hokkaido University, Sapporo 060-8628, Japan*

[2]*Department of Physics, Hokkaido University, Sapporo 060-0810, Japan*

[3]*Complex Matter Dept., Jozef Stefan Institute, Jamova 39, Ljubljana, SI-1000, Slovenia*

The quasiparticle (QP) dynamics with different symmetry is investigated in the superconducting (SC) and normal state of the high-temperature superconductor $Bi_2Sr_2CaCu_2O_{8+\delta}$ (Bi2212) using optical pump-probe experiments with different light polarizations at different doping levels. The observation of distinct selection rules for SC excitations present in A_{1g} and B_{1g} symmetries, and for the pseudogap (PG) excitations present in A_{1g} and B_{2g} symmetries by the probe, and absence of any dependence on the pump beam polarization leads to the unequivocal conclusion of the existence of a spontaneous spatial symmetry breaking in the PG state not limited to the sample surface.

I. INTRODUCTION

Ultrafast pump-probe spectroscopy has been widely used to investigate the high-T_c superconductivity from various viewpoints [1–5]. Nonequilibrium studies give a unique insight into quasiparticle (QP) dynamics, revealing universal two-component QP dynamics associated with the superconducting (SC) gap and pseudogap (PG) excitations in high-T_c materials. The two types of excitations were characterized by distinct relaxation times, temperature dependencies, and/or sign of the optical signal, depending on the material, doping level, photoexcitation intensity, and the wavelengths of light used in the pump-probe experiments [6–10]. The dependence on the probe photon polarization of the two-component reflectivity dynamics has also been reported [11,12]. However, the absence of a fundamental understanding of the optical processes involved in pump-probe experiments so far prevented analysis of the symmetry of excitations or detailed theoretical analysis of the excitations on a microscopic level. Here, by performing a concise symmetry analysis of pump-probe experiments on Bi2212 high temperature superconductors and identifying the processes involved, we open the way to investigations of hidden broken symmetry and local or mesoscopic symmetry breaking in systems with competing orders.

Generally pump-probe experiments can be described as a two step process. In the first step, the *pump* pulse excitation can be viewed as a process which can be divided into a coherent stimulated Raman excitation [13] and an incoherent dissipative excitation. In pseudotetragonal (D_{4h}) symmetry, considered appropriate for the cuprates [14], A_{1g} and A_{2g} as well as B_{1g} and B_{2g} excitations can be coherently excited by the coherent excitation process for the photon polarizations lying in the CuO_2 plane [15]. On the other hand, the dissipative excitation cannot coherently excite nonsymmetric modes. However, *an additional possibility exists*, where in the presence of a local, dynamic, or hidden symmetry breaking nonsymmetric modes can be excited coherently also by the totally symmetric dissipative excitation. This allows us to probe symmetry breaking by means of the pump-probe spectroscopy.

In the second step of the pump-probe experiment, the transient change of reflectivity ΔR detected by the probe can be described by the Raman-like process [13]. Assuming the pseudotetragonal structure (D_{4h} point group) for Bi2212, we can obtain the simple form of the angle dependence of the transient reflectivity (for details see the Supplemental Material [16]):

$$\Delta R(\theta) \propto \Delta R_{A_{1g}} + \Delta R_{B_{1g}} \cos(2\theta) + \Delta R_{B_{2g}} \sin(2\theta). \quad (1)$$

Here θ is defined in Fig. 1(a), and A_{2g} symmetry is omitted because it does not contribute in our experimental configuration. Thus, in principle, by measuring the angle dependence of $\Delta R(\theta)$ and using Eq. (1) we can separate the T-dependent QP dynamics associated with different symmetries and consequently identify the states involved [17].

Previous analysis in the cuprates have indicated that the electronic Raman scattering in the B_{2g} symmetry probes excitations in the nodal ($\pi/2,\pi/2$) direction in k space, while the B_{1g} scattering probes excitations in the antinodal directions ($\pi/2,0$) and ($0,\pi/2$) [15,18–20] as shown in Fig. 1(b). An A_{1g} symmetry component is also present, whose origin is still highly controversial [15]. Recent studies suggest the presence of the PG in the nodal direction [21] implying an s-wave symmetry, in contrast to the common assumption of a PG with nodes, indicating that the PG symmetry is still an open issue. Some important progress has been made on the broken symmetry of the PG in Bi2212 and related compounds [22–24]. A rotational broken symmetry of the PG in YBCO and LSCO has also been reported in the THz region very recently [25]. A detailed symmetry analysis of optical pump-probe experiments can therefore potentially give important new information on the symmetry, lifetime, and temperature dependence of nodal and anti-nodal excitations in the cuprates and other superconductors with an enhanced bulk sensitivity with respect to the time-resolved angle-resolved photoemission spectroscopy (ARPES) [2,4].

II. EXPERIMENT

The optical measurements were performed on freshly cleaved slightly overdoped (OD, $T_c \approx 82$ K) and underdoped (UD, $T_c \approx 69$ K) Bi2212 single crystals grown by the traveling solvent floating zone method. For optimal signal-to noise ratio we used a pump at $E_{pu} = 3.1$ eV ($\lambda_{pu} = 400$ nm) and
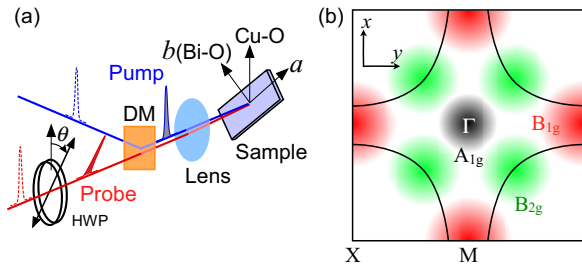
FIG. 1. (Color online) (a) A schematic illustration of the two-color pump-probe setup for polarization-resolved measurements. The probe ($\lambda_{pr} = 800$ nm) was variably polarized by a half-wave plate (HWP) and was combined with the pump ($\lambda_{pu} = 400$ nm) by a dichroic mirror (DM). The angle θ is measured relative to the Cu-O bond axes. (b) The k-space selectivity of the probe according to the Raman-like process is indicated [15].

probe at $E_{pr} = 1.55$ eV ($\lambda_{pr} = 800$ nm) from a cavity-dumped Ti:sapphire oscillator with a 120 fs pulses and a repetition rate of 270 kHz (to avoid heating). The pump and probe beams were coaxially overlapped by a dichroic mirror and focused to a 20 μm diameter spot on the ab plane of the crystal with an objective lens ($f = 40$ mm). Low-pass filters were used to suppress any remaining scattered pump beam. We use the notation where x and y point along the Cu-O bonds [Fig. 1(b)]. The sample orientation was checked by x-ray diffraction, in which the b axis is determined by the direction of the multiple peaks responsible for a one-dimensional (1D) superlattice modulation.

III. RESULTS

First we note that ΔR is found to be independent of the pump polarization within the experimental error of the measurements ($< \sim 2\%$), while the probe polarization dependence of ΔR is very temperature dependent.

The angular dependencies of ΔR at selected temperatures, obtained by rotating the probe polarization from $\theta = 0$ to $360°$ at each temperature, are presented in Figs. 2(a)–2(f) for OD and Figs. 2(g)–2(l) for UD samples, respectively. The upper panels (a)–(c) and (g)–(i) show the intensity plots of $\Delta R(\theta)$ together with the cross-sectional views at $\theta = 0°$. The polar plots (d)–(f) and (j)–(l) show the angular dependence of the signal amplitude $\Delta R(\theta)$.

At the lowest temperature, where the SC signal is dominant, $\Delta R(\theta)$ is slightly elliptic, with the long axis close to, but not coincident, with the Cu-O bonds direction [Figs. 2(a) and 2(d) and Figs. 2(g) and 2(j)]. The amplitude of the signal increases with increasing $\mathcal{F}$, showing saturation behavior near $\mathcal{F}_{th}^{SC} = 1$ μJ/cm^2 [26]. With increasing $\mathcal{F}$, an additional fast relaxation signal with opposite sign with respect to the SC signal appears, which persists above T_c and disappears around T^*. This component has been previously assigned to the PG QPs [8,27], where $T^* \simeq 140$ K for OD and 240 K for UD samples, respectively, and is consistent with previous measurements [28]. The reason for the PG signal appearing at higher $\mathcal{F}$ is that the PG component has a higher saturation threshold than the SC signal, and therefore becomes visible below T_c with increasing $\mathcal{F}$ [27].
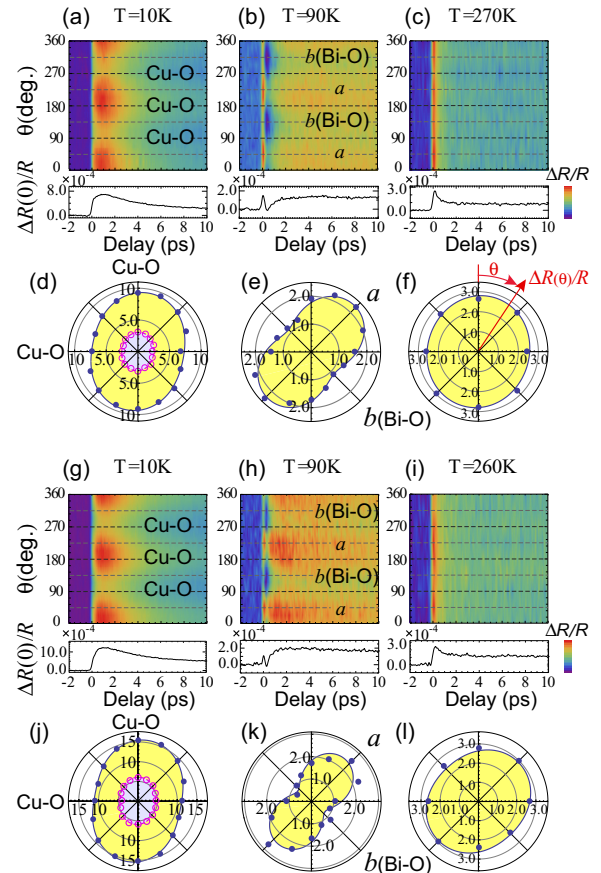
FIG. 2. (Color online) (a)–(c) and (g)–(i) $\Delta R(\theta)/R$ transients at typical temperatures for OD and UD samples, respectively. (d)–(f) and (j)–(l) Polar plots of the maximum values of $\Delta R(\theta)/R$ ($\times 10^4$). The solid lines indicate fits using Eq. (1). $\Delta R(\theta)/\Delta R$ at delay time of 10 ps is also shown (open circles with dashed fitting line) in (d) and (j). Note that the Cu-O bonds directions are drawn horizontal and vertical, while the crystalline axes are along the Bi-O bonds, and are rotated nearly $45°$ from the Cu-O bonds.

In the PG state above T_c, but below T^*, the long axis is oriented along the crystalline axes ($\theta \simeq 45°$) [Figs. 2(b) and 2(e) and Figs. 2(h) and 2(k)].

Above T^*, a signal with opposite sign to the PG (the same sign as SC) becomes visible, which has been attributed to the electron energy relaxation in the metallic state [29]. This high-temperature signal is almost independent of θ [Figs. 2(c) and 2(f) and Figs. 2(i) and 2(l)].

In Fig. 3 we present the T dependencies of the B_{1g}, B_{2g}, and A_{1g} components of ΔR obtained by fitting Eq. (1) to experimental data. The B_{1g} and B_{2g} components show clear dominance of the SC and PG responses, respectively. The B_{1g} component increases strongly below T_c, while above T_c it is consistent with the observed SC fluctuations [33]. On the other hand, the B_{2g} component shows a gradual decrease with increasing the temperature across T_c and a faster subpicosecond relaxation time, which is consistent with the general behavior observed for the PG QPs [6,32]. The difference of the T dependencies between OD and UD samples reflects the systematic variation of the gaps with the doping level.
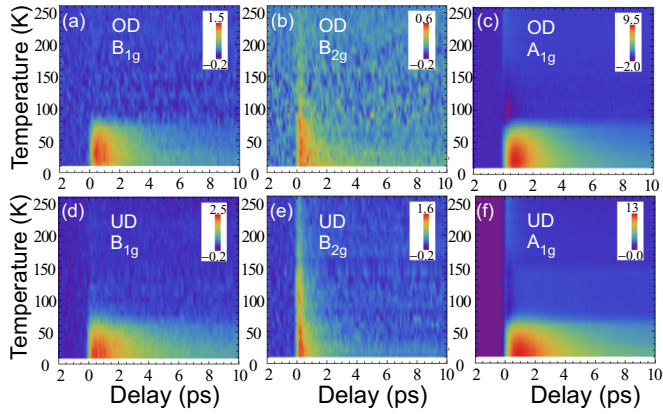
FIG. 3. (Color online) T dependencies of the B_{1g}, B_{2g}, and A_{1g} components of ΔR corresponding to SC, PG, and metallic state relaxation, respectively, for OD (top) and UD (bottom) samples. The values of the color bars indicate $\Delta R/R \times 10^4$.

In Fig. 4 we plot the amplitudes of different components for both OD and UD samples as a function of temperature. The B_{1g} and A_{1g} components show dominant intensity below T_c, and their T dependencies can be fit well using the Mattis-Bardeen formula [31,34]. The B_{2g} component can be fit well by the Kabanov's relaxation model [32,35] which gives a T-independent $\Delta_{PG} = 30$ meV for OD and $\Delta_{PG} = 41$ meV for UD samples. The values of Δ_{PG} in each sample are consistent with the values obtained from other experiments [36,37]. While the B_{1g} component shows a significant change at T_c, the B_{2g} component does not show any measurable change within the noise level.
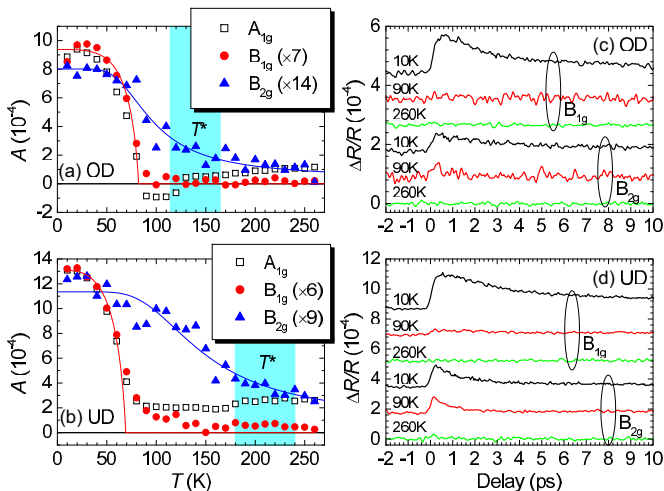
FIG. 4. (Color online) T dependencies of the A_{1g}, B_{1g}, and B_{2g} component amplitudes for UD and OD samples. Note that both B components begin to show an increase of the amplitude below T^*. T^*s obtained from tunneling [30] are within the region indicated by the shaded area. In the case of the A_{1g} symmetry the PG contribution is superimposed on top of the nearly temperature-independent signal, and has a negative sign. The solid and dashed lines are fits using Mattis-Bardeen [31] and Kabanov [32] models, respectively.

IV. DISCUSSIONS

The absence of any pump polarization anisotropy has important consequences. It rules out stimulated Raman excitation as the excitation mechanism for any nontotally-symmetric modes. At the same time, the fact that the B-symmetry responses are observed by the probe means that they are somehow excited by the pump pulse.

During the dissipative excitation, each high-energy QP created by a photon relaxes the excess energy independently by nonelastic scattering with emission of excitations of various symmetries. Due to the stochastic nature of the involved processes the phases of the created excitations are random so their modulation of the dielectric tensor cannot be detected coherently. At the same time, the state of the system is characterized by time-dependent scalar densities corresponding to different excitations, which can only couple to the totally symmetric representation of the dielectric tensor and coherently excite only the totally symmetric modes [38]. We are therefore left with the only remaining possibility that the B-symmetry modes are excited coherently because the underlying tetragonal point group symmetry is spontaneously broken below T^*.

Formally, B_{2g} symmetry breaking of the pseudotetragonal symmetry is already present at room temperature in Bi2212 due to the weak inherent orthorhombicity of the underlying crystal structure from the BiO chain modulation arising from the mismatch of Bi-O and Cu-O layers [39]. In the resulting D_{2h} point group symmetry the a and b axes are rotated at ~45° with respect to the Cu-O bonds. The presence of any coherent B_{1g} symmetry excitation, on the other hand, requires breaking of both the CuO$_2$ plane pseudotetragonal (D_{4h}) and D_{2h} symmetry down to C_{2h} [see Fig. 5(a)] [40].

In our data however, both symmetry breakings are suppressed at the room temperature appearing clearly below T^*, implying that the B_{2g} component is not simply a consequence of the underlying Bi2212 orthorhombicity. The data in Fig. 4
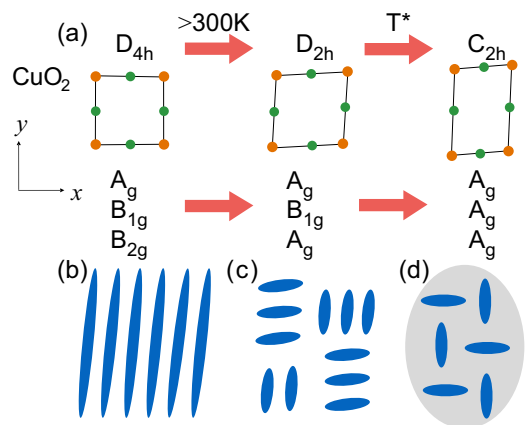
FIG. 5. (Color online) (a) The reduction of symmetries consistent with the observed polarization anisotropy. The CuO$_2$ layers are shown. Using the centrosymmetric refinement [39], the highest possible symmetry below T^* is C_{2h}. The relevant irreducible representations are given in each case. (b) Schematic representations corresponding to nematic ordering, (c) short stripe ordering [41–46], and (d) local polaronic order [47].

clearly show the B_{1g} symmetry breaking to occur slightly below T^* and clearly above T_c in both samples. Furthermore, while the BiO chain ordering discussed above can in principle cause the B_{2g} symmetry breaking effect it *cannot* cause the observed B_{1g} symmetry breaking neither above nor below T_c.

Despite the fact that the d-wave SC order parameter corresponds to B_{1g} symmetry, the observed effect cannot be linked directly to the symmetry of the SC order parameter. The SC order parameter is complex so any expansion of the dielectric constant in terms of the SC order parameter can only contain powers of $|\Delta_{SC}|^2$, which are of A_{1g} symmetry. This is consistent with the strong response of the SC state observed in the A_{1g} channel.

The appearance of the SC response in the B_{1g} symmetry can therefore only be associated with a preexisting underlying order oriented along the Cu-O bonds (see Fig. 5). This finding is consistent with previous scanning-tunneling microscopy (STM) measurements indicating the presence of stripe order oriented along one of the two orthogonal Cu-O bond directions on the crystal surface [41–44]. The magnitude of the B_{1g} component significantly exceeds 10% of the A_{1g} magnitude. Since the optical probe penetration depth is of order of 100 nm [27] this indicates that the stripe order and the B_{1g} component are not limited to the surface, but are present also in the bulk. The sensitivity of the B_{1g} component to the SC order also suggests that the instability towards formation of the stripe order and the superconductivity are intimately connected.

The distinct absence of the SC response in the B_{2g} channel is consistent with the sensitivity of the corresponding Raman vertex to the nodal ($\pi/2, \pi/2$) direction in the k space, where the SC gap has nodes. On the other hand, the presence of the PG response in B_{2g} channel indicates that the PG response can, at least in part, be associated with the nodal QPs. Remarkably this implies the presence of the PG in the nodal region, consistently with recent Raman results [21]. We note that this does not contradict the results of ARPES studies. However, in contrast to ARPES, pump-probe spectroscopy probes hundreds of nanometers in depth and detects also the unoccupied states. It suggests however, that the ARPES picture of the nodal region might be incomplete.

Upon reduction of symmetry from tetragonal to orthorhombic each of the B symmetry breakings of the fourfold axis can occur in two equivalent directions (e.g., along x or

along y). Since our experiment is stroboscopic and averages over many pulses B_{1g} and B_{2g} channels do not average out only if there exist an underlying anisotropy persisting between subsequent pulses separated by 4 μs, which aligns the symmetry breakings. This can be imposed by extrinsic defect structure or strain. In the case of Bi2212 it appears that that the anisotropy responsible for the B_{2g} channel alignment can originate in the weak orthorhombicity of the crystal, while the anisotropy responsible for the B_{1g} is of extrinsic origin amplified by the softness of the CuO_2 planes towards stripe ordering or similar textures.

The symmetry reduction and broken symmetry textures compatible with the observed symmetry breaking are shown schematically in Fig. 5. Assuming a homogeneous broken-symmetry state, the deformation would be uniform [Fig. 5 b)]. Alternatively, in an inhomogeneous state the observed anisotropy is consistent with a picture of locally ordered commensurate charge-density-wave (CDW) patches along the Cu-O bonds [48,49], nematic order [22,50,51], or stripe order with different size stripes [45–47]. Note that incommensurate CDW order would be expected to lead to further reduction in point group symmetry, beyond C_{2h}. In all such cases, the observed signal is a (nonzero) spatial average over different possible domain orientations shown schematically in Figs. 5(b)–5(d).

V. CONCLUSIONS

We conclude by noting that the presented symmetry analysis of the response observed in pump-probe spectroscopy opens up new possibilities for investigating the dynamics of spatial symmetry breaking, as well as the k-space anisotropy of electronic excitations beyond established methods like Raman and Kerr-effect spectroscopy, while offering a complementary information on unoccupied states and bulk properties compared to related new techniques such as time-resolved ARPES.

ACKNOWLEDGMENTS

[1] R. A. Kaindl, M. A. Carnahan, D. S. Chemla, S. Oh, and J. N. Eckstein, Phys. Rev. B **72**, 060510 (2005).

[2] L. Perfetti, P. A. Loukakos, M. Lisowski, U. Bovensiepen, H. Eisaki, and M. Wolf, Phys. Rev. Lett. **99**, 197001 (2007).

[3] D. Fausti, R. I. Tobey, N. Dean, S. Kaiser, A. Dienst, M. C. Hoffmann, S. Pyon, T. Takayama, H. Takagi, and A. Cavalleri, Science **331**, 189 (2011).

[4] J. Graf, C. Jozwiak, C. L. Smallwood, H. Eisaki, R. A. Kaindl, D. H. Lee, and A. Lanzara, Nat. Phys. **7**, 805 (2011).

[5] C. Giannetti, F. Cilento, S. Dal Conte, G. Coslovich, G. Ferrini, H. Molegraaf, M. Raichle, R. Liang, H. Eisaki, M. Greven, A. Damascelli, D. van der Marel, and F. Parmigiani, Nat. Commun. **2**, 353 (2011).

[6] J. Demsar, B. Podobnik, V. V. Kabanov, T. Wolf, and D. Mihailovic, Phys. Rev. Lett. **82**, 4918 (1999).

[7] P. Kusar, J. Demsar, D. Mihailovic, and S. Sugai, Phys. Rev. B **72**, 014544 (2005).

[8] Y. H. Liu, Y. Toda, K. Shimatake, N. Momono, M. Oda, and M. Ido, Phys. Rev. Lett. **101**, 137003 (2008).

[9] L. Stojchevska, P. Kusar, T. Mertelj, V. V. Kabanov, Y. Toda, X. Yao, and D. Mihailovic, Phys. Rev. B **84**, 180507 (2011).

[10] G. Coslovich, C. Giannetti, F. Cilento, S. Dal Conte, T. Abebaw, D. Bossini, G. Ferrini, H. Eisaki, M. Greven, A. Damascelli, and F. Parmigiani, Phys. Rev. Lett. **110**, 107003 (2013).

[11] D. Dvorsek, V. V. Kabanov, J. Demsar, S. M. Kazakov, J. Karpinski, and D. Mihailovic, Phys. Rev. B **66**, 020510 (2002).

[12] C. W. Luo, C. C. Hsieh, Y. J. Chen, P. T. Shih, M. H. Chen, K. H. Wu, J. Y. Juang, J. Y. Lin, T. M. Uen, and Y. S. Gou, Phys. Rev. B **74**, 184525 (2006).

[13] T. E. Stevens, J. Kuhl, and R. Merlin, Phys. Rev. B **65**, 144304 (2002).

[14] Conventionally the x an y axes are chosen along the Cu-O bond directions.

[15] T. P. Devereaux and R. Hackl, Rev. Mod. Phys. **79**, 175 (2007).

[16] See Supplemental Material at http://link.aps.org/supplemental/10.1103/PhysRevB.90.094513 for the probe angle-dependence of ΔR.

[17] Note that this symmetry analysis is valid also within the photoinduced absorption (PIA) picture commonly considered until now.

[18] S. Sugai and T. Hosokawa, Phys. Rev. Lett. **85**, 1112 (2000).

[19] R. Nemetschek, M. Opel, C. Hoffmann, P. F. Muller, R. Hackl, H. Berger, L. Forro, A. Erb, and E. Walker, Phys. Rev. Lett. **78**, 4837 (1997).

[20] N. Munnikes, B. Muschler, F. Venturini, L. Tassini, W. Prestel, S. Ono, Y. Ando, D. C. Peets, W. N. Hardy, R. Liang, D. A. Bonn, A. Damascelli, H. Eisaki, M. Greven, A. Erb, and R. Hackl, Phys. Rev. B **84**, 144523 (2011).

[21] S. Sakai, S. Blanc, M. Civelli, Y. Gallais, M. Cazayous, M. A. Measson, J. S. Wen, Z. J. Xu, G. D. Gu, G. Sangiovanni, Y. Motome, K. Held, A. Sacuto, A. Georges, and M. Imada, Phys. Rev. Lett. **111**, 107001 (2013).

[22] M. J. Lawler, K. Fujita, J. Lee, A. R. Schmidt, Y. Kohsaka, C. K. Kim, H. Eisaki, S. Uchida, J. C. Davis, J. P. Sethna, and E.-A. Kim, Nature (London) **466**, 347 (2010).

[23] Y. Kohsaka, T. Hanaguri, M. Azuma, M. Takano, J. C. Davis, and H. Takagi, Nat. Phys. **8**, 534 (2012).

[24] R.-H. He, M. Hashimoto, H. Karapetyan, J. D. Koralek, J. P. Hinton, J. P. Testaud, V. Nathan, Y. Yoshida, H. Yao, K. Tanaka, W. Meevasana, R. G. Moore, D. H. Lu, S.-K. Mo, M. Ishikado, H. Eisaki, Z. Hussain, T. P. Devereaux, S. A. Kivelson, J. Orenstein, A. Kapitulnik, and Z.-X. Shen, Science **331**, 1579 (2011).

[25] Y. Lubashevsky, L. D. Pan, T. Kirzhner, G. Koren, and N. P. Armitage, Phys. Rev. Lett. **112**, 147001 (2014).

[26] Note that the threshold is different than in Ref. [27] due to a different pump wavelength.

[27] Y. Toda, T. Mertelj, P. Kusar, T. Kurosawa, M. Oda, M. Ido, and D. Mihailovic, Phys. Rev. B **84**, 174516 (2011).

[28] T. Nakano, N. Momono, M. Oda, and M. Ido, J. Phys. Soc. Jpn. **67**, 2622 (1998).

[29] C. Gadermaier, A. S. Alexandrov, V. V. Kabanov, P. Kusar, T. Mertelj, X. Yao, C. Manzoni, D. Brida, G. Cerullo, and D. Mihailovic, Phys. Rev. Lett. **105**, 257001 (2010).

[30] R. Dipasupil, M. Oda, N. Momono, and M. Ido, J. Phys. Soc. Jpn. **71**, 1535 (2002).

[31] T. Mertelj, P. Kusar, V. V. Kabanov, L. Stojchevska, N. D. Zhigadlo, S. Katrych, Z. Bukowski, J. Karpinski, S. Weyeneth, and D. Mihailovic, Phys. Rev. B **81**, 224504 (2010).

[32] V. V. Kabanov, J. Demsar, B. Podobnik, and D. Mihailovic, Phys. Rev. B **59**, 1497 (1999).

[33] I. Madan, T. Kurosawa, Y. Toda, M. Oda, T. Mertelj, P. Kusar, and D. Mihailovic, Sci. Rep. **4**, 5656 (2014).

[34] D. C. Mattis and J. Bardeen, Phys. Rev. **111**, 412 (1958).

[35] V. V. Kabanov, J. Demsar, and D. Mihailovic, Phys. Rev. Lett. **95**, 147002 (2005).

[36] M. Oda, K. Hoya, R. Kubota, C. Manabe, N. Momono, T. Nakano, and M. Ido, Physica C **281**, 135 (1997).

[37] T. Kurosawa, T. Yoneyama, Y. Takano, M. Hagiwara, R. Inoue, N. Hagiwara, K. Kurusu, K. Takeyama, N. Momono, M. Oda, and M. Ido, Phys. Rev. B **81**, 094519 (2010).

[38] H. J. Zeiger, J. Vidal, T. K. Cheng, E. P. Ippen, G. Dresselhaus, and M. S. Dresselhaus, Phys. Rev. B **45**, 768 (1992).

[39] P. A. Miles, S. J. Kennedy, G. J. McIntyre, G. D. Gu, G. J. Russell, and N. Koshizuka, Physica C **294**, 275 (1998).

[40] In the 45° rotated Bi-2212 D_{2h} point symmetry the pseudotetragonal (D_{4h}) B_{1g} representation corresponds to the B_{1g} in D_{2h}. A B_{1g} symmetry breaking leads at least to lowering of the point symmetry from D_{2h} to C_{2h}.

[41] M. Vershinin, S. Misra, S. Ono, Y. Abe, Y. Ando, and A. Yazdani, Science **303**, 1995 (2004).

[42] C. Howald, H. Eisaki, N. Kaneko, M. Greven, and A. Kapitulnik, Phys. Rev. B **67**, 014533 (2003).

[43] Y. Kohsaka, C. Taylor, K. Fujita, A. Schmidt, C. Lupien, T. Hanaguri, M. Azuma, M. Takano, H. Eisaki, H. Takagi, S. Uchida, and J. C. Davis, Science **315**, 1380 (2007).

[44] K. M. Lang, V. Madhavan, J. E. Hoffman, E. W. Hudson, H. Eisaki, S. Uchida, and J. C. Davis, Nature (London) **415**, 412 (2002).

[45] T. Mertelj, V. V. Kabanov, and D. Mihailovic, Phys. Rev. Lett. **94**, 147003 (2005).

[46] T. Mertelj, V. V. Kabanov, J. M. Mena, and D. Mihailovic, Phys. Rev. B **76**, 054523 (2007).

[47] G. I. Bersuker and J. B. Goodenough, Physica C **274**, 267 (1997).

[48] S. Sugai, Y. Takayanagi, and N. Hayamizu, Phys. Rev. Lett. **96**, 137003 (2006).

[49] D. H. Torchinsky, F. Mahmood, A. T. Bollinger, I. Bozovic, and N. Gedik, Nat. Mater. **12**, 387 (2013).

[50] S. A. Kivelson, E. Fradkin, and V. J. Emery, Nature (London) **393**, 550 (1998).

[51] G. Seibold and J. Lorenzana, Phys. Rev. Lett. **94**, 107006 (2005).